FINITE ELEMENT MESHING FOR CARDIAC ANALYSIS*

Yongjie Zhang† Chandrajit Bajaj‡

Institute for Computational Engineering and Sciences
Department of Computer Sciences
The University of Texas at Austin

ABSTRACT

This application paper presents details of the technique we developed to produce an adaptive and quality tetrahedral finite element mesh model of a human heart. Beginning from a polygonal surface model consisting of twenty-two components, we first edit and convert it to volumetric gridded data. A component index for each cell edge and grid point is computed for assisting the boundary and material layer detection. Next we extract adaptive and quality tetrahedral meshes from the volumetric gridded data using our Level Set Boundary and Interior-Exterior (LBIE) Mesher. The mesh adaptivity is controlled using a feature sensitive error function. Multiple layers with different materials were identified and meshed. Furthermore, one of the heart valves in the input multi-component surface model was replaced. The extracted final tetrahedral mesh is being utilized in the analysis of cardiac fluid dynamics via finite element simulations.

Keywords: cardiac model, tetrahedral mesh, boundary detection, material layer.

1. INTRODUCTION

A good geometric model of the human heart is important for the simulation of the human cardiovascular system, which is useful for medical education and the predictive medicine applications in cardiovascular surgery. Finite element analysis is an important method used for the simulation. Therefore, adaptive and quality tetrahedral finite element meshes of the cardiac model are required.

There are three main problems in the tetrahedral mesh generation for the cardiac model:

1. Model acquisition — model editing and volumetric gridded data calculation.
2. Adaptive and quality tetrahedral mesh extraction from volumetric gridded data.
3. Boundary and material layer detection.

The polygonal cardiac model from New York University's School of Medicine as shown in Figure 2, which was designed through collaboration between consultant cardiologists and graphical designers for interactive learning and virtual reality teaching aids, provides a good approximation of a normal adult heart. This human cardiac model has four chambers, five valves and all the major blood vessels. However, users may have some additional requirements for the cardiac model. For example, the valve connecting the left and right atriums was placed there to represent a 'foramen ovale' which is present in the embryo but not in the newborn, so it should be removed in studying the blood circulatory system of an adult. Small gaps between valve leaflets are required by some fluid dynamics software. The ventricular boundaries, detected from MRI scan data by segmentation techniques, can also be used in the model editing to build a patient-specific cardiac model. Therefore, we need to construct a user-specific geometric solid model by editing the virtual cardiac model.

The cardiac model can be decomposed into twenty-two components as shown in Figure 1. After model editing, we convert the edited polygonal model to the volumetric gridded data by using the signed distance method. We calculate a component index for each cell edge which will be used to decide the boundary index for each vertex in the extracted mesh. We also compute a component index for each grid point, which will help to detect multiple material layers.

We have extended the dual contouring isosurface extraction method [1] to adaptive and quality tetrahedral mesh generation, and developed a software named LBIE-Mesh (Level Set Boundary and Interior-Exterior

*http://www.ices.utexas.edu/∼jessica/paper/heart

†jessica@ices.utexas.edu
‡bajaj@cs.utexas.edu

Mesher) [2] [3]. The extended dual contouring method is chosen to generate finite element meshes for the cardiac model because this method takes isosurfaces as boundary surfaces and can generate meshes for complicated structures. The mesh adaptivity is controlled by a combination of major areas and the feature sensitive error function described in [2] [3]. We generate fine meshes in the regions of heart valves because they are important structures in fluid dynamics simulation. The feature sensitive error function can detect surface topology changes, and efficiently control the mesh adaptivity. Since the cardiac model has thin walls, modifications are made in the tetrahedral mesh extraction algorithm for thin structures.

In the boundary condition assignment of finite element simulations, users need to find all the boundary vertices lying on a certain component of the cardiac model such as the aorta. The component index is computed for each cell edge to help identify a boundary index for each vertex in the extracted mesh indicating the component to which it belongs.

The constructed tetrahedral mesh of the cardiac model can be used in the predictive treatment for the replacement of heart valves. In this situation, the heart valve and the myocardium have different material properties. Therefore, multiple material layers exist. The component index for each grid point helps to detect the interface between material layers.

The remainder of this paper is organized as follows: Section 2 summarizes the related previous work; Section 3 discusses the model editing and volumetric data generation; Section 4 explains the adaptive and quality tetrahedral mesh extraction from volumetric data; Section 5 describes how to generate boundary indices for boundary vertices; Section 6 talks about how to construct tetrahedral meshes in the region with multiple material layers; Section 7 shows some results and discusses other possible requirements for the cardiac model; the final section gives our conclusions.

2. PREVIOUS WORK

Cardiac Simulation: The simulation of cardiac fluid dynamics becomes more and more important because of its applications in medical education and predictive medicine for cardiovascular disease. A human heart surface model is simulated and constructed for studying cardiac fluid mechanics [4]. Mooney et. al [5] constructed a volumetric model for the human heart based on a polygonal model from New York University's School of Medicine, and produced a real-time simulation of the 3D phenomenon of the electrocardiogram. Hunter et. al [6] [7] [8] constructed a pig cardiac model and studied mechanics properties of the heart. Computational tools are used to construct patient-specific models based on CT and MRI scan data, which helps make alternate treatment plans for an individual patient. A model of blood vessels was constructed, and the blood flow inside them was simulated by studying fluid dynamics for cardiovascular disease [9] [10] [11] [12] [13]. Segmentation techniques are used to detect the boundaries of ventricles and 3D boundary element models of the heart are constructed from cine MRI scan data [14] [15] [16].

Tetrahedral Mesh Generation: Octree based, advancing front based and Delaunay-like techniques for tetrahedral mesh generation are reviewed in [17] and [18]. The octree technique recursively subdivides the cube containing the geometric model until the desired resolution is reached [19]. Advancing front methods start from a boundary and move a front from the boundary towards empty space within the domain [20] [21]. The Delaunay criterion is called 'empty sphere', which means that no node is contained within the circumsphere of any tetrahedra of the mesh. Different approaches of Delaunay refinement to define new nodes were studied [22] [23]. Sliver exudation [24] was used to eliminate slivers. Shewchuk [25] solved the problem of enforcing boundary conformity by constrained Delaunay triangulation.

The Marching Cubes algorithm (MC) [26] visits each cell in a volume and performs local triangulation based on the sign configuration of the eight vertices. The enhanced distance field representation and the extended MC algorithm [27] can detect and reconstruct sharp features in the isosurface. A surface wave-front propagation technique [28] is used to generate multiresolution meshes with good aspect ratio. MC [26] was extended to extract tetrahedral meshes between two isosurfaces from volume data [29]. Nielson proposed a different algorithm for interval volume tetrahedralization [30]. The dual contouring isosurface extraction method [1] has been extended to adaptive and quality tetrahedral mesh generation [2] [3]. [31] proposed an algorithm to triangulate a d-dimensional region with a bounded aspect ratio. Since many 3D objects are sampled in terms of slices, Bajaj et. al introduced approaches to construct triangular and tetrahedral meshes from the slice data [32] [33].

Algorithms for mesh improvement can be classified into three categories as reviewed in [17] and [18]: local refinement/coarsening by inserting/deleting points, local remeshing by face/edge swapping and mesh smoothing by relocating vertices. Laplacian smoothing, in its simplest form, relocates the vertex position at the average of the nodes connecting to it. This method generally works well for meshes in convex regions. However, it can result in distorted or even inverted elements near concavities in the mesh. Field [34] constrained the node movement in order to avoid the creation of inverted elements. Instead of relocating vertices based on a heuristic algorithm, people utilized an optimization technique, which measures the quality of the surrounding elements to a node and attempts to optimize it. The optimization-based smoothing yields better results while it is more expensive than Laplacian smoothing. Therefore, [35] [36] [37] recommended a combined Laplacian/optimization-based approach.

3. MODEL ACQUISITION

In this section, our goal is to construct a user-specific geometric solid model by editing a polygonal cardiac model (Figure 2), then converting it into volumetric

Boundary Index	Components	Color	Boundary Index	Components	Color
0	interior	–	12	valve of foramen ovale	green
1	aortic valve	blue	13	valve of foramen ovale	red
2	aortic valve	purple	14	right ventricle	blue
3	aortic valve	green	15	left ventricle	green
4	mitral valve	red	16	right atrium	red
5	mitral valve	yellow	17	right pulmonary v.	red
6	pulmonary valve	orange	18	inferior vena cava	orange
7	pulmonary valve	blue	19	left atrium	orange
8	pulmonary valve	red	20	right pulmonary a.	dark red
9	tricuspid valve	green	21	aorta	blue
10	tricuspid valve	purple	22	outer surface	pink
11	tricuspid valve	pink			

Figure 1: The corresponding relationship between the component/boundary index, cardiac components and their colors. The cardiac model is decomposed into twenty-two components as shown in Figure 2.

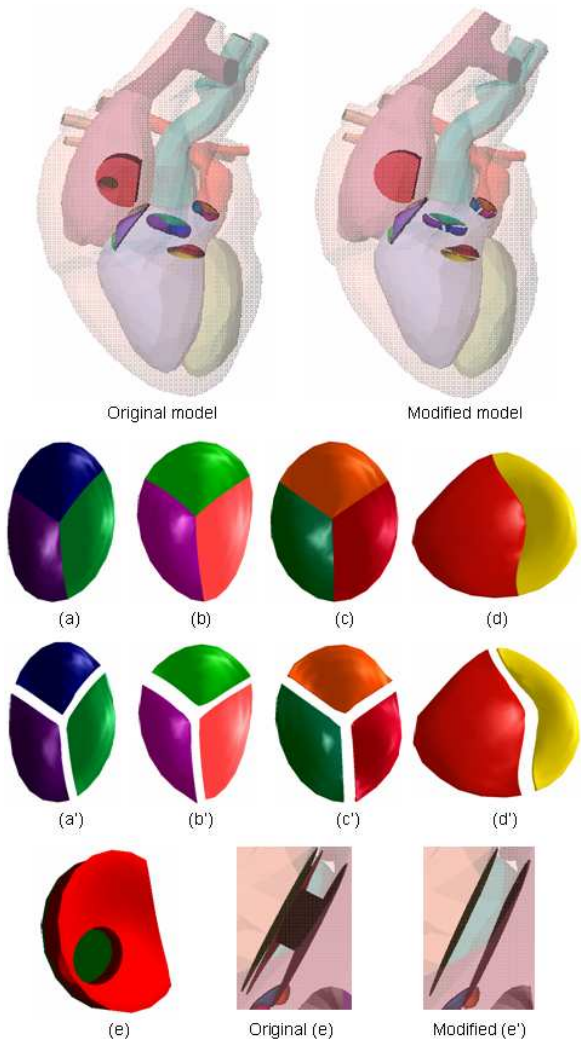

Figure 2: The original heart model from NYU* and the modified model. (a) - the aortic valve; (b) - the tricuspid valve; (c) - the pulmonary valve; (d) - the mitral valve; (a') (b') (c') and (d') - modified valves; (e) - the 'foramen ovale' connecting the left and right atriums. The original (e) and modified (e) are compared in the bottom row. Note*: With permission of New York University, Copyright 1994-2004.

gridded data using the signed distance method. The cardiac model is decomposed into twenty-two components as shown in Figure 1, and additional volume data indicating which component each grid point and each cell edge belong to is also calculated.

3.1 Model Editing

The heart plays an important role in the blood circulatory system of the human body. When one studies the blood flow in the heart, one is interested in how its muscular contractions pump blood around the body. There are two main pumping chambers that contract nearly simultaneously in a healthy heart. One is the left ventricle, which accepts oxygen-enriched blood from the lungs and pumps it to the body. The other is the right ventricle, which accepts oxygen-depleted blood from the body and pumps it to the lungs. Therefore, no connective valve between the left and right atriums is necessary in studying the blood circulatory system, and the 'foramen ovale' connecting the two atriums as shown in Figure 2(e) needs to be removed from the original model.

We first remove the valve connecting the left and right atriums in the virtual heart model, and fill the holes in the two atriums (Figure 2(e)). There are four important valves left consisting of two or three leaflets (Figure 2(a $\sim$ d)). In our finite element model of the human heart, the aortic valve, the tricuspid valve, the pulmonary valve and the mitral valve should have gaps between its cuspid components since blood flows through them in the circulatory system. The gaps are small, and no blood may pass through when the valves are closed. Here Maya [38], a CAD software, is used to modify the original valve models to obtain gaps (Figure 2 (a' $\sim$ d')).

3.2 Volumetric Data Calculation

For each grid point in the volumetric gridded data, we calculate the shortest distance from this grid point to the edited polygonal cardiac model, and assign a sign to it indicating if this grid point lies inside the heart volume or not. Besides this, we also need to know which component of the cardiac model each grid

point and each cell edge belong to. Therefore, there is a value (the component index) attached at each cell edge, and a vector tagged at each grid point in the generated volumetric data containing the signed distance value and the component index.

For each cell edge, we find the component index of the triangle in the edited polygonal model which intersects this edge. The component index of each cell edge, especially the component index of each sign change edge, will be used to decide the boundary index for each boundary vertex in extracted meshes which helps assign boundary conditions in finite element simulations.

When we calculate the component index for each grid point, we first find the triangle in the polygonal model which is the closest to this grid point, and get the index number of the component containing this triangle from Figure 1. If this triangle belongs to more than one component, then this grid point lies in their shared plane or shared line. The component index for each grid point needs to be kept in the volumetric data, and will be used to detect material layers in the extracted meshes. In the heart model with the replaced mitral valve, there are two different material types. One is the heart tissue, the other is the material of the replaced mitral valve. For a grid point, if its closest triangle belongs to the mitral valve in the polygonal model, then the material index is 1, otherwise it is 0. The material index for each boundary vertex in extracted meshes is helpful to assign material properties in finite element simulations.

4. TETRAHEDRAL MESHING

In this section, we are going to construct an adaptive tetrahedral heart model with all necessary components, such as arteries, veins, four chambers, and four heart valves. We choose the extended Dual Contouring method to construct the tetrahedral heart model from volumetric gridded data [2] [3] because it takes isosurfaces as boundaries and can generate adaptive and quality meshes for complicated structures.

4.1 Mesh Extraction

The dual contouring method [1] uses an octree-based data structure, and analyzes those edges whose endpoints lie on different sides of the isosurface, called *sign change edges*. The mesh adaptivity is achieved during a top-down octree construction. Each sign change edge is shared by either four (uniform case) or three (adaptive case) cells, and one minimizer is calculated for each of them by minimizing a predefined Quadratic Error Function (QEF). For each sign change edge, a quadrilateral or triangle is constructed by connecting the minimizers. These quadrilaterals and triangles provide a 'dual' approximation of the isosurface.

The dual contouring method has already been extended to tetrahedral mesh generation from volumetric data [2] [3]. In this scheme, cells containing the isosurface are called boundary cells, and interior cells are those cells whose eight vertices are inside the isosurface. In the process of tetrahedral mesh extraction, all

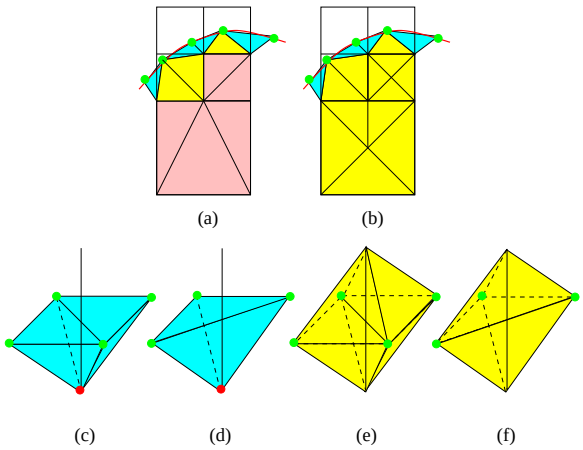

Figure 3: 2D triangulation and 3D tetrahedralization. (a) - the 2D scheme used in [2] [3]; (b) - our 2D scheme. (c $\sim$ f) - our 3D schemes: (c)(d) - sign change edge; (e)(f) - interior edge. The green solid points represent minimizer points, and the red solid points represent the interior vertex of the sign change edge.

boundary cells and interior cells should be analyzed. There are two kinds of edges in boundary cells, one is a sign change edge, the other is an interior edge. Interior cells only have interior edges. In [2] [3], interior edges and interior faces in boundary cells are dealt with in a special way, and the volume of the interval volume inside boundary cells is tetrahedralized. For interior cells, we only need to split them into tetrahedra. Figure 3(a) shows a 2D example.

Here we adopt a slightly different algorithm, in which we do not distinguish between boundary cells and interior cells when we analyze them. We only consider two kinds of edges — sign change edges and interior edges. For each boundary cell, we can obtain a minimizer point by minimizing its Quadratic Error Function. For each interior cell, we set the center point of the cell as its minimizer point. In 2D (Figure 3(b)), there are two cells sharing each edge, and two minimizer points are obtained. For each sign change edge, the two minimizers and the interior vertex of this edge construct a triangle (blue). For each interior edge, each minimizer/center point and this edge construct a triangle (yellow). In 3D (Figure 3(c $\sim$ f), there are three or four cells sharing each edge. Therefore, the three (or four) minimizers and the interior vertex of the sign change edge construct one (or two) tetrahedron (blue tetrahedra), while the three (or four) minimizers and the interior edge construct two (or four) tetrahedra (yellow tetrahedra).

Compared with the algorithm presented in [2] [3], this method is simpler and easier to implement. The two methods are actually the same if the interval volume is thin, while this method will generate a little more tetrahedra for thick interval volume.

4.2 Mesh Adaptivity and Topology

In order to keep all the features of the complicated human heart model, and at the same time minimize

the number of elements for efficient finite element calculation, we choose adaptive tetrahedral meshes.

The mesh adaptivity can be controlled by important regions and by a feature sensitive error function defined in [2] [3]. First we find out the regions of four heart valves, then refine the octree cells in these important regions and generate fine meshes, while keep coarse meshes in other areas. The feature sensitive error function measures the difference of the isosurfaces between coarse and fine levels, and it can detect geometric and topological features sensitively. If the error function value of an octree cell is greater than a predefined threshold ε, then this cell should be refined and finer meshes will be generated.

If a non-manifold situation happens in the finest resolution, then the local topology is wrong. We use the subdivision method [3] to solve this problem. A trilinear function is constructed to represent the true topology, and we keep splitting the octree cell until each subcell contains only one component of the isosurface.

5. BOUNDARY DETECTION

We assign the boundary index for each interior vertex of the interval volume in extracted meshes to be 0, and what we are interested in is how to decide the boundary index for each boundary vertex. In the process of Dual Contouring isosurface extraction, we analyze each sign change edge. Four or three minimizer points are generated, and their boundary indices are assigned the same with the component index of this sign change edge (green and blue minimizers in Figure 4(a)). If a minimizer point is assigned by different boundary indices when analyzing various sign change edges, then this minimizer point lies in the shared region of multiple components (red minimizers in Figure 4(a)).

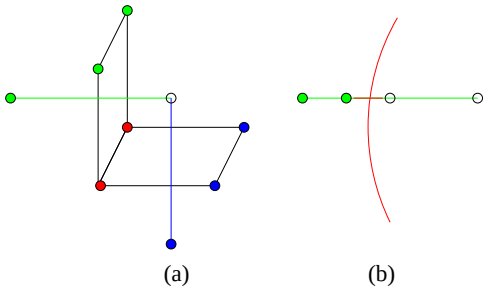

Figure 4: Boundary detection - (a) There are two sign change edges, the green edge and the blue one, belonging to two different cardiac components. The red minimizers lie in the shared region of the two components. (b) Minimal sign change edge (the red edge) is chosen for the boundary detection.

Minimal edges are defined as edges of leaf cells that do not contain an edge of a neighboring leaf. We always choose the minimal sign change edges to detect the boundary index since it is closer to the isosurface and provides more accurate boundary information. In Figure 4(b), the red curve represents the real isocontour, the green edge is the sign change edge and the short red edge is the minimal sign change edge. When we detect the boundary index, we should choose the component index number of the red edge instead of that of the green edge.

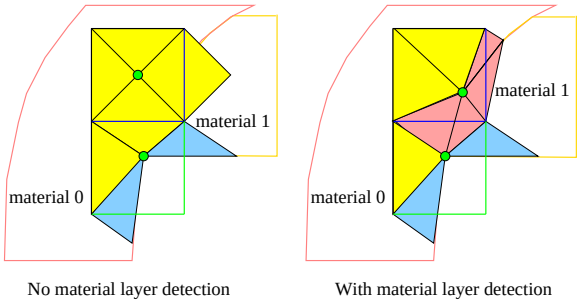

Figure 5: 2D Triangulation of the region without/with material layer detection. There are two materials (0 and 1) in this example. The top cell is an interior cell and the bottom cell is a boundary cell. The green edges are sign change edges, and the blue edges were interior edges, but are set as sign change edges considering the material properties. The green points are minimizer points.

6. MATERIAL LAYER DETECTION

We need to detect various material layers when the object consists of multiple materials. For example, the mitral valve is one of the most easily injured valves for elderly people, and it needs to be replaced in the treatment for some patients. The replaced mitral valve has different material properties from the myocardium. Therefore the interface between the myocardium and the replaced mitral valve needs to be detected.

In the process of tetrahedral mesh extraction from volumetric gridded data, we need to analyze both boundary cells and interior cells. For interior cells, if there are multiple materials in it, then we can not set the cell middle point as the minimizer point. For example, there are two different materials (0 and 1) in an interior cell, then we negate the function value of grid points with material 1 while keep the function value of grid points with material 0. A minimizer point can be calculated using the same Quadratic Error Functions in the cell whose grid points are tagged with new function values. For all analyzed (boundary or interior) cells, we first check if all the eight grid points belong to the same material. If not, we need to re-consider the interior edge whose two endpoints have different materials as a sign change edge.

Figure 5 shows a 2D example, two blue interior edges should be re-analyzed. The left picture shows the triangular mesh generated without the material layer detection, while the right one shows the mesh with the material layer detection. In the right picture, two blue triangles are generated for green sign change edges, three yellow triangles are generated for interior edges and four pink triangles are generated for blue sign change edges. It is obvious that the interface between the two material regions is preserved by pink triangles.

	Vertex Number	Tetra Number	Extraction Time (ms)	Edge-ratio (best, worst)	Joe-Liu (best, worst)	Volume (minimal, maximal)
Heart^b	148516	728321	11253	(1.02, 1.20×10^5)	(1.0, 1.23×10^{-4})	(4.88×10^{-8}, 2.56×10^2)
Heart^a	146163	715795	-	(1.02, 8.5)	(1.0, 2.04×10^{-2})	(4.35×10^{-4}, 4.33×10^2)

Figure 6: The comparison of the three quality criteria (the edge-ratio, the Joe-Liu parameter and the minimal volume) before/after the quality improvement for the human heart model. Heart^b - before quality improvement; Heart^a - after quality improvement. Meshes are extracted from a volumetric gridded data of 257^3.

7. RESULTS AND DISCUSSION

We have developed an interactive program for adaptive and quality tetrahedral mesh extraction and rendering of the cardiac model based on our meshing software LBIE-Mesh. Our results were computed on a PC equipped with a Pentium III 800MHz processor and 1GB main memory.

The adaptive tetrahedral meshes shown in Figure 7 are extracted from a volumetric gridded data of signed distance function with the resolution of 257^3. The mesh adaptivity is controlled by important regions (four valves) and a feature sensitive error function. It is obvious that the finest meshes are generated in the regions of the aortic valve, the tricuspid valve, the pulmonary valve and the mitral valve. Figure 8 shows the four valves and their valve gaps in the extracted tetrahedral mesh. Geometric and topological features such as structures with thin walls as shown in Figure 7(c) are identified by the feature sensitive error function, and adaptive meshes are generated to represent the heart model with correct topology.

In our output, we provide not only the geometric position of each vertex and the connectivity information for each tetrahedron, but also the location information of each vertex with a boundary index and the material information with a material index. We use a different color to represent each component of the cardiac model. The corresponding relationship between the component/boundary index, cardiac components and the color map is listed in Figure 1. The boundary index assists the boundary condition assignment, and the material index helps assign material properties in finite element simulations. Figure 7(b) shows the detected twenty-two components of the cardiac model in wireframe. Various leaflets of the four heart valves are identified with different color as shown in Figure 8. In a cardiac model with the replace mitral valve as shown in Figure 9, the interface between the mitral valve and the myocardium is detected after the material layer detection.

As described in [3], we also adopted the edge-ratio, the Joe-Liu parameter and the minimal volume as our quality metrics, and used the edge contraction and smoothing method to improve the mesh quality. Figure 6 shows the mesh size, the extraction time and the improvement of the three quality metrics. The extraction time includes octree traversal, quadratic error function computation and actual mesh extraction. It is obvious that the worst values of the edge-ratio, the Joe-Liu parameter and the minimal volume were improved significantly.

In the process of finite element simulations, people may need anisotropic meshes in some regions of the cardiac model. For example, finer meshes is required along the gradient direction of finite element solutions, while meshes stretch in the tangential directions. In some thin structures, the extracted meshes may have only one element in the thickness direction. However the finite element solution has strong gradient across it, which requires the mesh must have multiple elements through the thin structure to capture these gradients. Therefore, it is desirable to generate anisotropic meshes with multiple elements through the thickness that are stretched in the tangential direction. One way for anisotropic mesh generation is to find the shortest path from a boundary vertex to its opposite boundary surface along the thickness direction, identify the edges to be refined in the extracted tetrahedral mesh, and refine the tetrahedral mesh along it by inserting extra points at the middle of edges.

8. CONCLUSION

In this paper, we have constructed a user-specific cardiac solid model by editing an educational polygonal surface model, converted it into volumetric gridded data of the signed distance function, and generated adaptive and quality tetrahedral finite element meshes for it. Each of the twenty-two components is identified and represented by a different color, and the interface of the material layer between the replaced mitral valve and myocardium is detected. For each boundary vertex in the extracted meshes, a boundary index and a material index are provided to assist the assignment of boundary conditions and material properties in finite element simulations.

Quantization of ventricular mass and function are important in myocardial diseases, so it is important to detect boundaries of ventricles from MRI scan data. With the development of scanning and segmentation techniques, MRI scan data will be used to construct a patient-specific cardiac solid model. Then we can generate adaptive and quality finite element meshes for each specific patient with boundary and material layer detection.

ACKNOWLEDGEMENTS

We thank Bong-Soo Sohn and Karlapalem L. Chandrasekhar for the using of their signed distance function calculation code, Zeyun Yun for useful discussion, Fred Nugen for proofreading, Jianguang (Jason) Sun for the system management and NYU for providing access to the polygonal surface mesh of the heart model

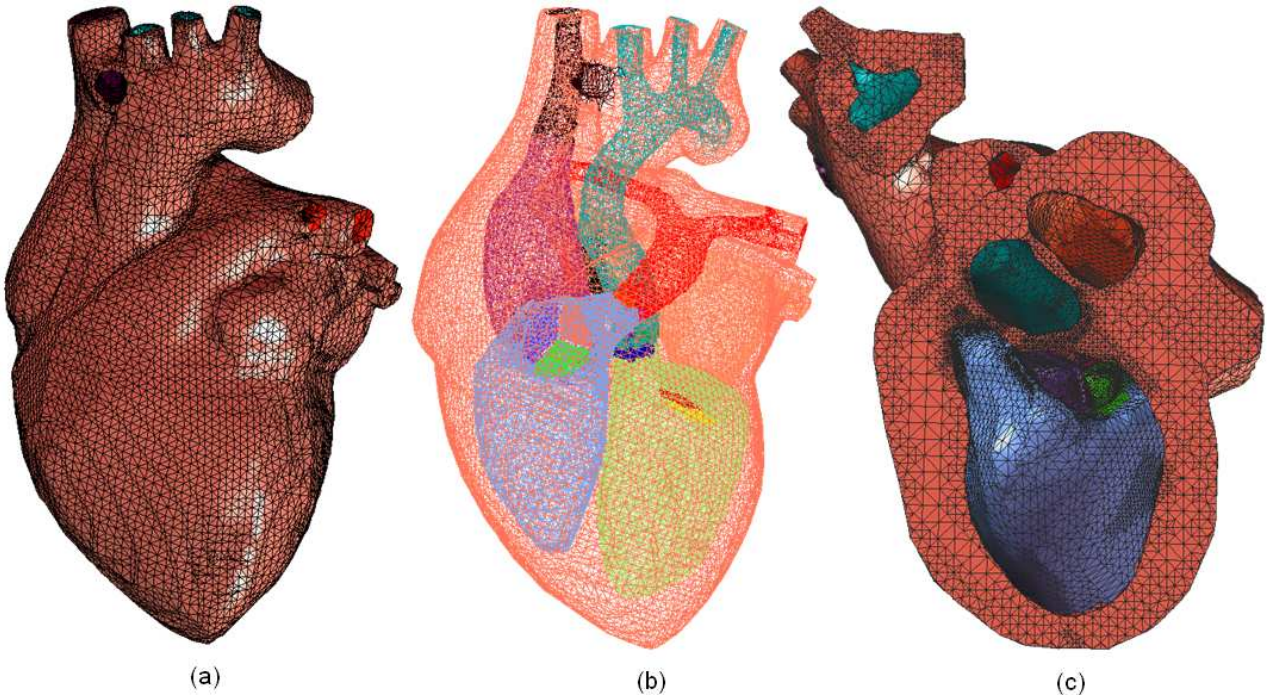

Figure 7: Adaptive tetrahedral meshes for the heart model. (a) - the heart model viewed from outside; (b) - the result of boundary detection in wireframe, each of the twenty-two components of the heart model is represented by a different color, the relationship between the color and heart components is listed in Figure 1; (c) - a cross section of the adaptive tetrahedral mesh, it is obvious that the valves have the finest mesh, thin structures are identified by the feature sensitive error function, and adaptive meshes are generated to preserve correct topology.

(With permission of New York University, Copyright 1994-2004). This work was supported in part by NSF grants ACI-0220037, CCR-9988357, EIA-0325550, a UT-MDACC Whitaker grant, and a subcontract from UCSD 1018140 as part of the NSF-NPACI project, Interaction Environments Thrust.

References

[1] Ju T., Losasso F., Schaefer S., Warren J. "Dual Contouring of Hermite Data." *Proceedings of SIGGRAPH 2002*, pp. 339–346. 2002

[2] Zhang Y., Bajaj C., Sohn B.S. "Adaptive and Quality 3D Meshing from Imaging Data." *ACM Symposium on Solid Modeling and Applications. Seattle, WA.*, pp. 286–291. 2003

[3] Zhang Y., Bajaj C., Sohn B.S. "3D Finite Element Meshing from Imaging Data." *Submitted to the special issue of Computer Methods in Applied Mechanics and Engineering (CMAME) on Unstructured Mesh Generation, www.ices.utexas.edu/∼jessica/meshing.* 2003

[4] McQueen D.M., Peskin C.S. "A three-dimensional computer model of the human heart for studying cardiac fluid dynamics." *ACM SIGGRAPH Computer Graphics*, vol. 34, pp. 56–60. 2000

[5] Mooney R., Sullivan C.O., Ryan J., Bell C. "The Construction of a Volumetric Cardiac Model for Real-time ECG Simulation." *Poster Sessions of the Winter Conference on Computer Graphics.* 2003

[6] Smith N.P., Pullan A.J., Hunter P.J. "An Anatomically Based Model of Coronary Blood Flow and Myocardial Mechanics." *SIAM Journal of Applied Mathematics*, vol. 62, 990–1018, 2002

[7] Smith N.P., Mulquiney P.J., Nash M.P., Bradley C.P., Nickerson D.P., Hunter P.J. "Mathematical modelling of the heart: cell to organ." *Chaos, Solitons and Fractals*, vol. 13, no. 8, 1613–1621, 2003

[8] Stevens C., Remme E., LeGrice I., Hunter P.J. "Ventricular mechanics in diastole: material parameter sensitivity." *Journal of Biomechanics*, vol. 36, 737–748, 2003

[9] Taylor C.A., Hughes T.J.R., Zarins C.K. "Finite Element Modeling of Blood Flow in Arteries." *Computer Methods in Applied Mechanics and Engineering*, vol. 158, 155–196, 1998

[10] Taylor C.A., Draney M.T., Ku J.P., Parker D., Steele B.N., Wang K., Zarins C.K. "Predictive Medicine: Computational Techniques in Therapeutic Decision Making." *Computer Aided Surgery*, vol. 4, no. 5, 231–247, 1999

[11] Wang K.C., Dutton R.W., Taylor C.A. "Level Sets for Vascular Model Construction in Computational Hemodynamics." *IEEE Engineering in Medicine and Biology*, vol. 18, no. 6, 33–39, 1999

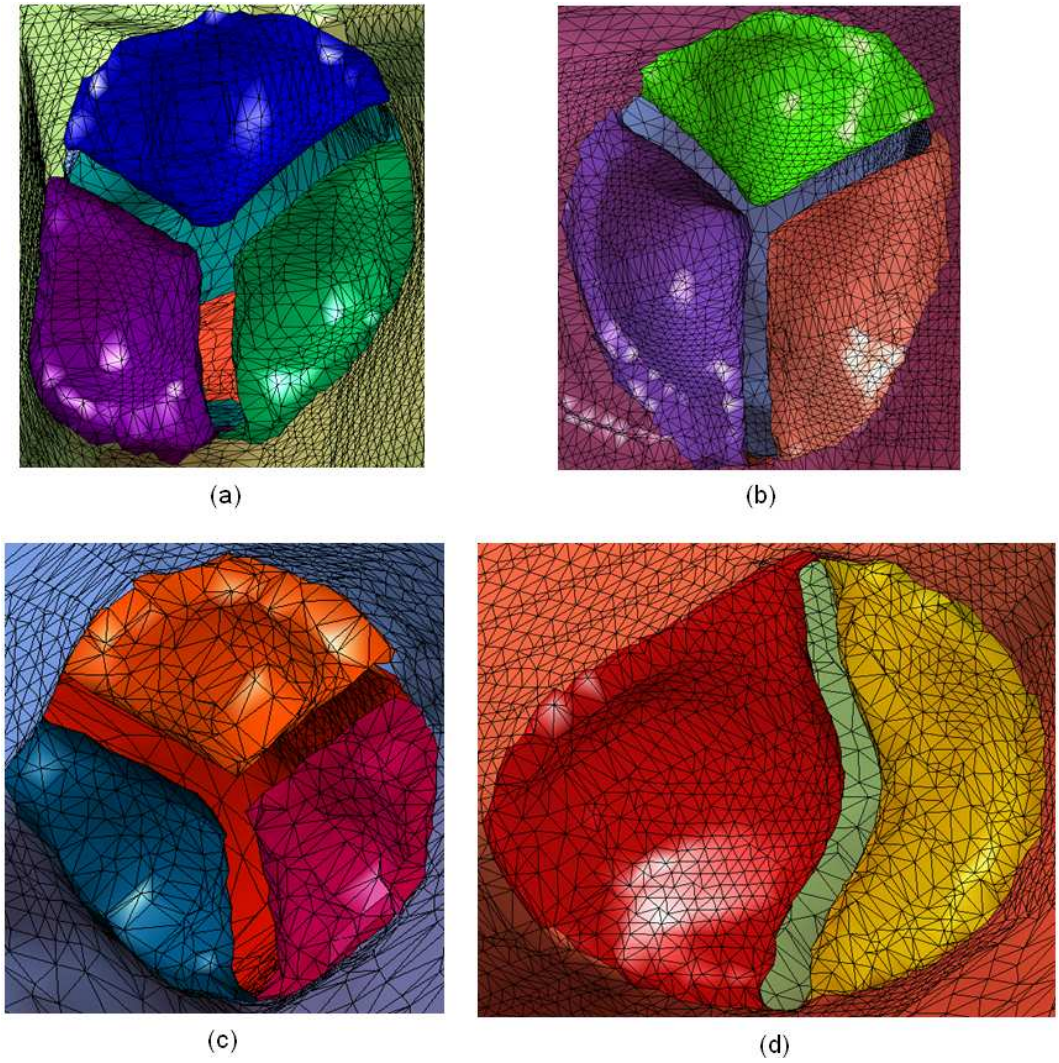

Figure 8: Four valves with gaps in the adaptive tetrahedral mesh of the cardiac model, the relationship between the color and heart components is listed in Figure 1. (a) - the aortic valve; (b) - the tricuspid valve; (c) - the pulmonary valve; (d) - the mitral valve.

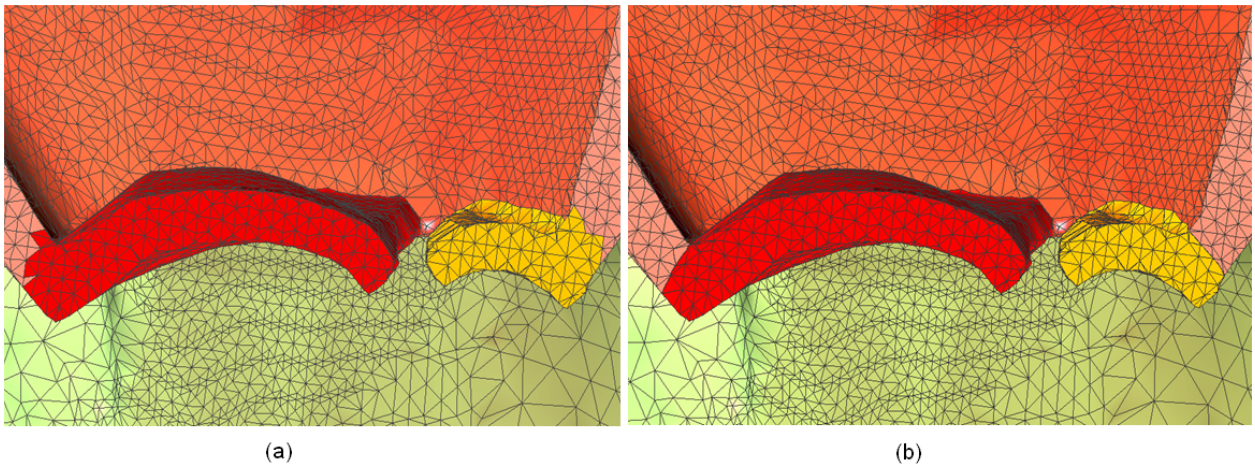

Figure 9: The result of material layer detection in the extracted tetrahedral meshes – the interface between the mitral valve and the myocardium is identified. The corresponding relationship between the color map and the components is listed in Figure 1. (a) - a cross section of the mitral valve before material layer detection; (b) - a cross section of the mitral valve after material layer detection.

[12] Wan J., Steele B.N., Spicer S.A., Strohband S., Feijoo G.R., Hughes T.J., Taylor C.A. "A One-Dimensional Finite Element Method for Simulation-Based Medical Planning for Cardiovascular Disease." *Computer Methods in Biomechanics and Biomedical Engineering*, vol. 5, 195–206, 2002

[13] Ku J.P., Draney M.T., Arko F.R., Lee W.A., Chan F.P., Pelc N.J., Zarins C.K., Taylor C.A. "In Vivo Validation of Numerical Prediction of Blood Flow in Arterial Bypass Grafts." *Annals of Biomedical Engineering*, vol. 30, 743–752, 2002

[14] Zhukov L., Bao Z., Guskov I., Wood J., Breen D. "Dynamic Deformable Models for 3D MRI Heart Segmentation." *SPIE Medical Imaging*, pp. 1398–1405. 2002

[15] Niessen W.J., van Bemmel C.M., Caregnato A.F., Siers M.J.A., Wink O. "Model-based segmentation of cardiac and vascular images." *IEEE*, pp. 22–25. 2002

[16] Veister H., Ltjnen J., Katila T. "Creating 3D boundary element models of the heart from 2D projections." *Biomag*, pp. 821–824. 2000

[17] Teng S.H., Wong C.W. "Unstructured mesh generation: Theory, practice, and perspectives." *International Journal of Computational Geometry and Applications*, vol. 10, no. 3, 227–266, 2000

[18] Owen S. "A survey of unstructured mesh generation technology." *7th International Meshing Roundtable*, pp. 26–28. 1998

[19] Shephard M.S., Georges M.K. "Three-Dimensional mesh generation by finite octree technique." *International Journal for Numerical Methods in Engineering*, vol. 32, 709–749, 1991

[20] Frey P.J., Borouchaki H., George P.L. "Delaunay tetrahedralization using an advancing-front approach." *5th International Meshing Roundtable*, pp. 31–48. 1996

[21] Seveno E. "Towards an adaptive advancing front method." *6th International Meshing Roundtable*, pp. 349–362. 1997

[22] Chew L.P. "Guaranteed-quality Delaunay meshing in 3D (short version)." *13th ACM Symposium on Computational Geometry*, pp. 391–393. 1997

[23] Cheng S.W., Dey T.K. "Quality Meshing with Weighted Delaunay Refinement." *Proc. 13th ACM-SIAM Sympos. Discrete Algorithms (SODA)*, pp. 137–146. 2002

[24] Cheng S.W., Dey T.K., Edelsbrunner H., Facello M.A., Teng S. "Sliver Exudation." *Proc. Journal of ACM*, vol. 47, 883–904, 2000

[25] Shewchuk J.R. "Constrained Delaunay Tetrahedrizations and Provably Good Boundary Recovery." *11th International Meshing Roundtable*, pp. 193–204. 2002

[26] Lorensen W.E., Cline H.E. "Marching Cubes: A High Resolution 3D Surface Construction Algorithm." *Proceedings of SIGGRAPH*, pp. 163–169. 1987

[27] Kobbelt L., Botsch M., Schwanecke U., Seidel H. "Feature Sensitive Surface Extraction from Volume Data." *Proceedings of SIGGRAPH*, pp. 57–66. 2001

[28] Wood Z., Desbrun M., Schroder P., Breen D. "Semi-Regular Mesh Extraction from Volumes." *Visualization Conference Proceedings*, pp. 275–282. 2000

[29] Fujishiro I., Maeda Y., Sato H., Takeshima Y. "Volumetric Data Exploration Using Interval Volume." *IEEE Transactions on Visualization and Computer Graphics*, vol. 2, no. 2, 144–155, 1996

[30] Nielson G.M., Sung J. "Interval Volume Tetrahedrization." *IEEE Visualization*, pp. 221–228. 1997

[31] Mitchell S.A., Vavasis S.A. "Quality Mesh Generation in Higher Dimensions." *SIAM Journal on Computing*, vol. 29, no. 4, 1334–1370, 2000

[32] Bajaj C., Coyle E., Lin K.N. "Arbitrary Topology Shape Reconstruction from Planar Cross Sections." *Graphical Modeling and Image Processing*, vol. 58, no. 6, 524–543, 1996

[33] Bajaj C., Coyle E., Lin K.N. "Tetrahedral Meshes from Planar Cross Sections." *Computer Methods in Applied Mechanics and Engineering*, vol. 179, 31–52, 1999

[34] Field D.A. "Laplacian smoothing and Delaunay triangulations." *Communications in Applied Numerical Methods*, vol. 4, 709–712, 1988

[35] Canann S.A., Tristano J.R., Staten M.L. "An approach to combined Laplacian and optimization-based smoothing for triangular, quadrilateral and quad-dominant meshes." *7th International Meshing Roundtable*, pp. 479–494. 1998

[36] Freitag L.A. "On combining Laplacian and optimization-based mesh smoothing techniqes." *AMD-Vol. 220 Trends in Unstructured Mesh Generation*, pp. 37–43, 1997

[37] Freitag L., Ollivier-Gooch C. "Tetrahedral mesh improvement using swapping and smoothing." *International Journal for Numerical Methods in Engineering*, vol. 40, 3979–4002, 1997

[38] "Instant Maya 5, a software application for 3D digital animation and visual effects." *www.aliaswavefront.com*